



Analysis of X-ray images and spectra (aXis2000): A toolkit for the analysis of X-ray spectromicroscopy data

Adam P. Hitchcock

Chemistry & Chemical Biology, McMaster University, Hamilton, ON, Canada

ARTICLE INFO

Keywords:

Spectromicroscopy data analysis package
aXis2000
STXM
Chemical mapping
Polarization mapping

ABSTRACT

Spectromicroscopy refers to analytical methods that combine imaging and spectroscopy to provide detailed, spatially resolved analytical information about a sample, such as the type and quantitative spatial distributions of chemical components, geometric or magnetic alignment information, crystal structure, etc. The analysis of X-ray images and spectra (aXis2000) software described in this work provides a set of routines within a single, integrated, graphical-oriented package to read, display, manipulate and analyze spectromicroscopy data, with particular focus on soft X-ray spectromicroscopy methods such as scanning transmission X-ray microscopy (STXM), X-ray photoemission electron microscopy (XPEEM), scanning photoelectron X-ray microscopy (SPEM) and transmission X-ray microscopy (TXM). Here, this free software is described and compared to other software that can provide similar or complementary capabilities. Examples of spectromicroscopic analyses using advanced features of aXis2000 are provided.

1. Introduction

The pace of research in many areas of science, engineering and technology is accelerating, in part because of advances in analytical techniques, such as the various branches of electron and X-ray spectromicroscopy. Incredible improvements have been made in instrumentation such as higher brightness synchrotrons, more sophisticated electron microscopes, improved optics and detectors, and new techniques (e.g. coherent diffraction techniques such as ptychography). In order to take full advantage of these advances, it is essential to have software that can efficiently and accurately extract useful information from spectromicroscopy data sets. I started research in instrumentation and applications of scanning transmission X-ray microscopy (STXM) in 1994 during a sabbatical year at the Advanced Light Source (ALS, Lawrence-Berkeley National Laboratory, Berkeley, CA). At that time there were a number of software routines for STXM data analysis, many written by Chris Jacobsen and his group to support researchers using STXM at NSLS-I. Those routines were generally in the form of Interactive Data Language (IDL) [1] scripts. The code would often need to be modified in order to analyze new data sets or types of data. There was no unifying graphical user interface (GUI). For researchers who used STXM frequently and analyzed STXM data on a near daily basis, these scripts were adequate; indeed, having to modify code regularly gave students and postdoctoral fellows useful skills. However for occasional users, or

even frequent users who would have long periods of time between measurements, it was a challenge to learn or relearn IDL syntax and routines at each data analysis session. I personally was frustrated by this, so in ~1998 I took it upon myself (with lots of help from my son, Peter) to write aXis2000, a GUI for STXM data analysis. Initially, most of the content was the routines written by Chris Jacobsen and his group members. A standardized GUI was implemented. The package was first shared in ~1998, and was named aXis2000 at the start of the present millennium. As the true power of spectromicroscopy based on near edge X-ray absorption spectroscopy (NEXAFS) stacks [2–6] became apparent, novel capabilities for stack analyses were developed. It became clear that the data processing capabilities of aXis2000 would be useful in a wide range of spectromicroscopies including the three other main soft X-ray microscopies - X-ray photoemission electron microscopy (XPEEM), scanning photoelectron X-ray microscopy (SPEM) and transmission X-ray microscopy TXM). Over time the input options have extended to a number of other spectromicroscopy techniques such as FTIR microscopy and TEM-EELS.

For well established methods, particularly those based on commercial instrumentation, it is common to define data analysis in terms of a workflow. However, in situations such as synchrotron-based spectromicroscopy, where new and modified methods are developed on a regular basis, it is useful to have a more flexible approach, with a GUI which has the ability to explore alternative data analysis approaches in

E-mail address: aph@mcmaster.ca.

<https://doi.org/10.1016/j.elspec.2023.147360>

Received 8 May 2023; Received in revised form 10 June 2023; Accepted 13 June 2023

Available online 24 June 2023

0368-2048/© 2023 The Author. Published by Elsevier B.V. This is an open access article under the CC BY-NC-ND license (<http://creativecommons.org/licenses/by-nc-nd/4.0/>).

Table 1
Summary of spectromicroscopy data analysis software packages.

| Name | ref. | website | GUI ? | Language | Data types | Strengths |
|---------------|-----------|---|-------|---------------|--|--|
| aXis2000 | This Work | http://unicorn.mcmaster.ca/axis/aXis2000-download.html | Y | IDL | STXM (all), PEEM (many), SPEM, TXM, FTIR | Unified, GUI-based tool kit |
| Mantis | [10] | https://spectromicroscopy.com/ | Y | Python | STXM - SDF, NeXus | Unsupervised statistical analysis; compressed sensing tomography |
| Stack_Analyze | | (available in aXis2000) | Y | IDL | STXM (NSLS-1, SDF) | Jacobsen routines from 2015 |
| STXMPy | [41] | (STXMPy source) | N | Python | STXM | Scripts for spectral analysis |
| STACKLab | [42] | (StackLab source) | N | Python | STXM | |
| STXM_Reader | [43] | (STXM_Reader source) | Y | LabView | STXM | |
| TXMWizard | [44] | https://sourceforge.net/projects/txm-wizard/ | Y | MatLab | TXM | XRF, stitching images, XANES |
| DAWN | [45] | https://dawnsci.org/ | Y | Eclipse, Java | PEEM, STXM | Diamond Light Source GDA based |
| ImageJ | [8] | https://imagej.nih.gov/ij/index.html | Y | Java | Need plug-ins | |
| PyMCA | [46] | http://pymca.sourceforge.net/ | Y | Python | TXM, nanoprobe | XRF spectral fitting & mapping |
| GG Macros | [47] | https://home.physics.wisc.edu/gilbert/software/ | N | IgorPro8 | XPEEM, STXM | Polarization contrast (PIC) mapping |
| Dada | [48] | | Y | HTTP | STXM, SAXS | High through put data analysis |

STXMPy source: <http://www.rzuser.uni-heidelberg.de/~ge6/Programing/STXMPy.html>

StackLab source: <https://www.mathworks.com/matlabcentral/fileexchange/24006-stxm-data-analysis-script-collection-stacklab>

STXM_Reader source: <https://drive.google.com/drive/folders/1cPFyfENvWmH4MBo0uuLz2IoW3QIPwG6?lf>

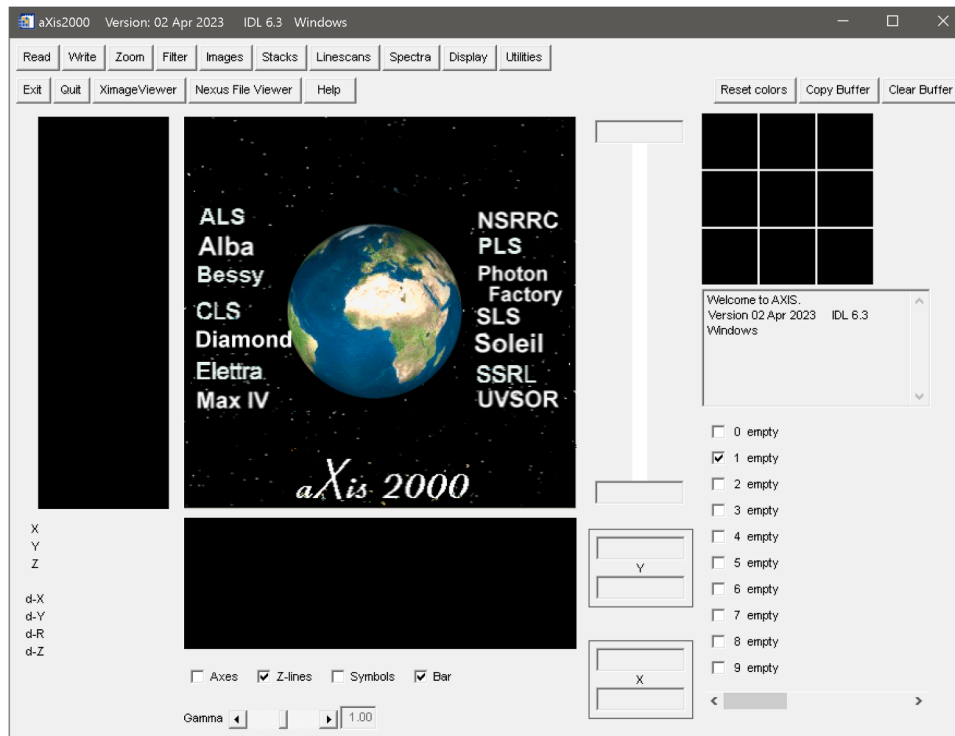


Fig. 1. aXis2000 home screen. The names of, or abbreviations for the synchrotron facilities are linked to websites for beamlines where aXis2000 is used for data analysis. The aXis2000 label is linked to the home page for aXis2000, which can be used to access the manual and a set of procedural documents, check for updates the software, etc.

order to find an optimal procedure. Also, in many measurements there are artifacts which require manual guidance to work around. For these situations, a toolkit approach such as aXis2000, can be more useful than a strict workflow approach. While aXis2000 has a broader goal, sequences of procedures can be combined, either manually, or by creating a macro, in order to construct a workflow for a specific type of analysis. Many of these work-flow like procedures are defined in the axis2000 manual (available as part of the [supplemental information](#) (axis2000_manual.pdf)). The pdf manual is also built into the code, and can be accessed by the help button on the main panel, and on the aXis2000 website [<http://unicorn.mcmaster.ca/aXis2000.html>].

While IDL was used as the computer language mainly for historic reasons, it is a very good choice for scientific data processing, especially those requiring extensive manipulation of multi-dimensional arrays, such as the $I(x,y,E)$ 3D stacks [3] which are often used in X-ray spectromicroscopy, and $I(x,y,E,X)$ 4D stacks, where X is an additional parameter such as sample angle (spectro-tomography or spectro-laminography), X-ray fluorescence energy (XRF-yield), sample modification parameter (magnetic field, voltage, T, etc), time, etc. IDL provides fast, efficient array processing, with often no need to use loop structures. It is very flexible in terms of implementation – either as an interpreted, scripting language or as a compiled program. IDL has

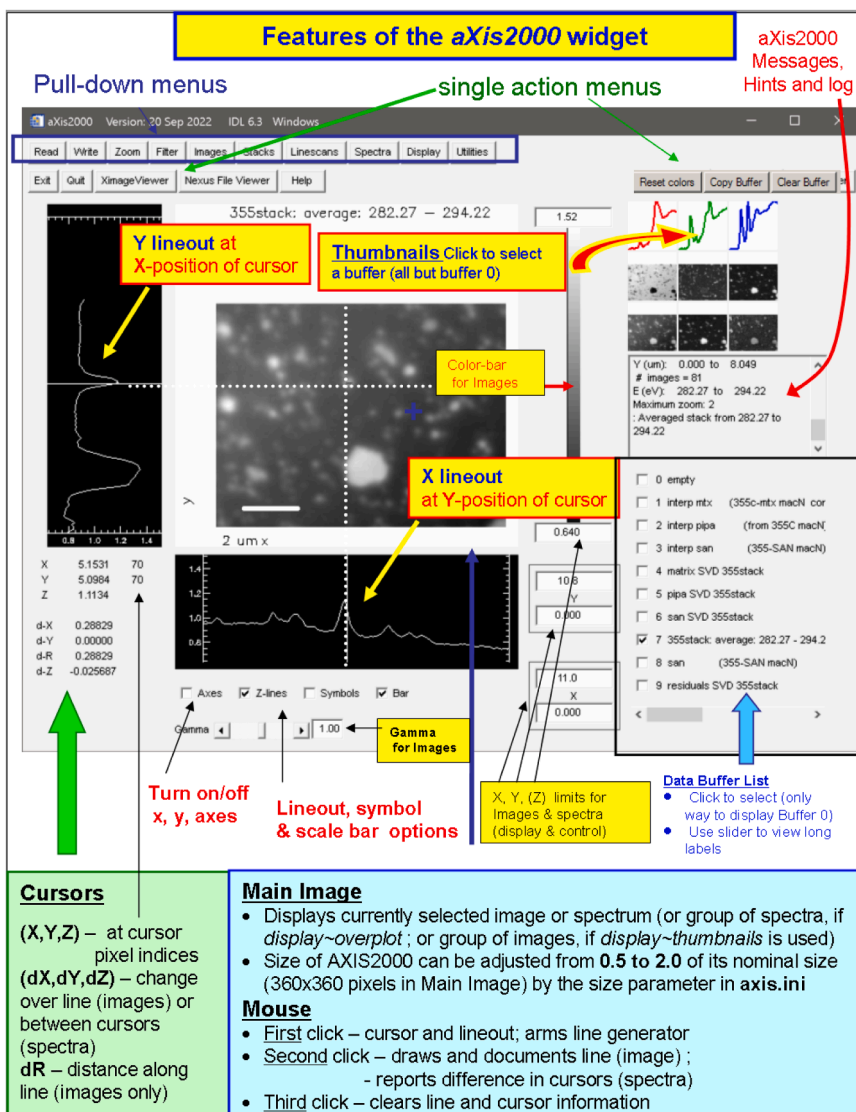


Fig. 2. aXis2000 main widget (graphical user interface, GUI), with labels identifying the various parts of the widget.

excellent documentation, often with references to standard texts on scientific computing (e.g. Numerical Recipes in C [7]). There are a large number of higher level routines written in IDL, for most of which the IDL code is provided. There is also an excellent website for requesting help and sharing code among the IDL user community (www.l3harrisgeospatial.com/Support/Forums/aff/217), as well as a number of IDL reference books. An IDL feature I find very useful as compared to many other languages, is that the latest version (at the time of writing, IDL version 8.9) supports legacy code so one is not forced to update code unnecessarily. IDL is the language used in many areas of scientific hyperspectral image analysis (astronomy, environmental remote sensing, medical etc). It is fully supported cross-platform (Windows, Unix, MacOS). Finally, using the IDL Virtual Machine approach, it is possible to make packages like aXis2000 shareable with others without requiring them to purchase a license or to learn anything about the IDL language.

aXis2000 is not the only software for spectromicroscopy data analysis. Table 1 lists other software packages that provide similar or complementary capabilities for analysis of X-ray and other spectromicroscopies. In many cases (STXMPy, StackLab, Dawn, etc) the software is a set of scripts, which require additional programming to use. In some cases there is no single unifying GUI, as in aXis2000 and Mantis, but rather ‘pop-up’ GUI interfaces for specific tasks.

The most general spectromicroscopy processing tool is ImageJ [8] (<https://imagej.nih.gov/ij/index.html>), a suite of Java routines supported by the US National institutes of Health (NIH). ImageJ can do all that aXis2000 can do, and much, much more. There is a large community providing custom ImageJ routines, including ones contributed by the STXM community such as the ScatterJn routine [9], which classifies spatially resolved analytical microscopy data to identify correlations in the spatial distributions of spectral signals.

Mantis, a Multivariate Analysis Tool for Spectromicroscopy [10] is a python based, workflow-oriented package for STXM stack analysis, with excellent capabilities. As with aXis2000, Mantis can read STXM stacks written in both the text-based self-defining format (SDF) written by the STXM_control acquisition & control program, and the NeXus hdf5 format (<http://www.nexusformat.org/>) used by the Pixelator STXM data acquisition. The formal definition of required content and internal organization of NeXus hdf5 files is described in [11]. Mantis can visualize, align, convert to optical density (OD), and, at the core of the software, perform advanced multivariate statistical analysis (MSA) for unsupervised processing of spectromicroscopy data. While emphasizing rigorous statistical approaches (principle component analysis, clustering, target analysis, etc), Mantis does have the capability to do least squares fitting (LSF) analyses using singular valued decomposition (SVD). It is also able to analyse 4D spectro-tomography data using a very

McMaster University

Hitchcock Group

aXis 2000 - Analysis of X-ray Images and Spectra.

last updated: 02 Jan 2023

Welcome to the home page of **aXis2000**.

The latest version of this IDL widget is **02 Jan 2023**

[Download aXis2000](#)

Instructions to get, install & run

[IDL Virtual Machine](#) versions of aXis2000

[Changes from previous version](#) (20 Sep 2022)

If you want the help file of the package: ([pdf](#))
If you want details of the code: ([html](#))

[Instructions to INSTALL or upgrade from old versions of aXis2000](#)

[Windows](#)

[OLD VERSIONS](#) (in case things you use stop working after updating !)

Some tutorials are available to guide users through specific procedures:

[simple-tutorial](#) [advanced-tutorial](#) [stack_fit](#)

Software I find very helpful to use in combination with aXis2000 on Windows for Win7 or Win8 you will need to set properties to 32-bit (MWsnap) or 16-bit (PaintShop4) to run

[MWsnap](#) [PaintShop4](#)

This package was developed and is maintained by *Adam Hitchcock* (1997..).
It contains code contributions from many people including:
Chris Jacobsen, Peter Hitchcock, Carl Zimba, Billy Loo, Eli Rotenberg, Jonathan Denlinger, Rick Kneidler, Jacob Stewart-Ornstein, Goran Johansson, Ivaylo Koprinarov, Florian Meirer, Dieter Ingerle, Ben Watts

© 2023 A.P. Hitchcock / McMaster University - All Rights Reserved
web site design by Christopher Amis (2002). Last updated on 2 Jan 2023 (aph)

Fig. 3. aXis2000 home page - <http://unicorn.mcmaster.ca/aXis2000.html>.

dose- and time-efficient compressed sensing algorithm [12]. The spectro-tomography tool in Mantis has the novel feature of being able to extract spectroscopic signals corresponding to irregular shaped, discontinuous regions of a 3D model, which can be useful to verify the spectral basis for a 3D spectro-tomography analysis.

In the following sections, I describe the architecture and menu structure of aXis2000.

(Section 2.1), and how to download and run aXis200 (Section 2.2). I then provide examples of applying aXis2000 to STXM data processing, including: conversion of a transmission image stack to chemical maps using internal and external reference spectra, and confirming the validity of the fit (Section 3.2); analysis of linear dichroic 3D data set $I(x, y, \theta_{\text{polarization}})$ (Section 3.3); analysis of a 4D $(x, y, E_{\text{in}}, E_{\text{out}})$ X-ray fluorescence yield NEXAFS data set (Section 3.4); and automated analysis of sets of closely related 3D stacks to make “STXM-chemi-movies” (Section 4.1).

2. Description of aXis2000

2.1. Layout of GUI

Fig. 1 is the home screen for aXis2000 when run in Windows OS. The aXis2000 package can also be run under Unix and MacOS operating systems, if the appropriate IDL package is installed. In addition to the

central image/ spectral display area of aXis2000, the home screen contains single-click and pull-down menus which are described briefly below and in more detail in the aXis2000 manual (in the [supplemental material](#)) or accessed by the ‘help’ button. The facility names listed on the home screen are internet links to the web pages of X-ray microscopy facilities where staff and users are using aXis2000 for data analysis.

Fig. 2 describes the different parts of the aXis2000 widget at the “block” level (‘widget’ is the IDL term for a graphical user interface, GUI). The *aXis2000-manual.pdf* distributed as part of the aXis2000 package, contains a brief description of each menu item, down to the lowest level of the many-layered pull-down menus. It also gives pictures and descriptions of secondary widgets that are created when executing functions such as data read-in, stack processing etc. The *aXis2000-manual.pdf* file also contains selected examples of data processing. These and many other examples, are described in a workflow manner, on the aXis2000 web page [<http://unicorn.mcmaster.ca/aXis2000.html>].

The top level of the pull down menus define either data processing functions (Read, Write, Zoom, Filter, Display, Utilities) or processing tools for each of the 4 types of spectromicroscopy data – 2-d Images, $I(x, y)$; 3-d Stacks, $I(x, y, E)$; 2-d Linescans, $I(r, E)$; and 1-d Spectra, $I(E)$. The central plotting area can display either 1-d or 2-d data. For 2D data, the side panels show line profiles along the y (left) and x (bottom) axes at the position of the cursor. Thus for linescans, where the horizontal axis is energy (E) and the vertical axis is distance along a line (R), the bottom

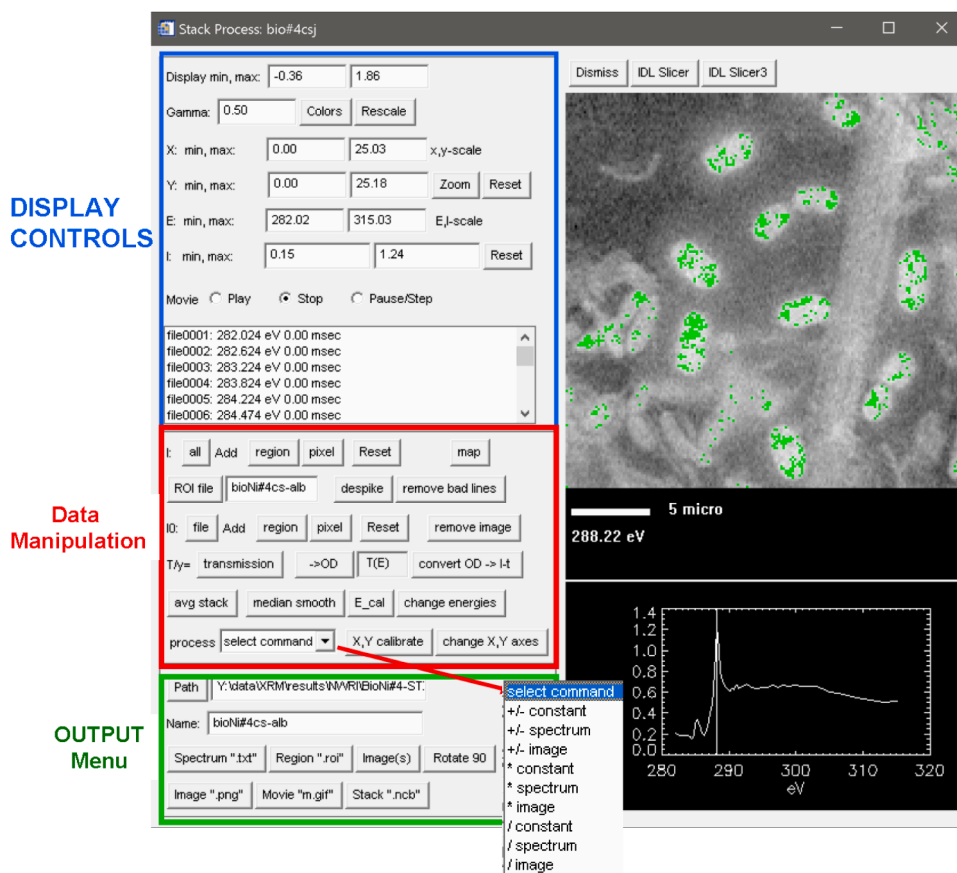


Fig. 4. Screen shot of the stack_process widget (*stacks~Analyse~stack process*). This highly functional widget is used to visualize and process stacks, $I(x,y,E)$.

panel displays spectra and the left panel displays intensity along the line at the (E,r) cursor position. Since many spectromicroscopies have a calibrated, reproducible spatial co-ordinate system, often defined using interferometry, absolute (x,y) co-ordinates are stored with the standard aXis2000 image data format (*.axb), and labeled x and y axes can be displayed by clicking on the Axes button at the bottom of the display. The display without labeled x and y axis (Axes button turned off) is more useful for screen capture to put images into reports and publications.

aXis2000 has nine 'permanent' buffers (1–9) and one 'working' buffer (0), where 'buffer' is a data entity. Each of the 10 buffers can hold 1-D data (e.g. spectra, line profiles, histograms, etc), 2D data (images, linescan-spectra, masks, etc) and limited types of 3D data (color coded composites; multi-dimensional). Whenever the content of a buffer is changed, (e.g. by one of the processing actions under the Images, Linescans or Spectra menus) the modified data is placed in buffer 0. If the user wishes to retain the modified data they should move the result from buffer 0 to one of the permanent buffers. (Note, buffer 0 can only be selected from the list of the headers of the 10 buffers, which is located below the information panel, to the right of the data display). Small images ('thumbnails') are plotted in a 3×3 array at the upper right of the main panel. In addition to displaying the content of buffers 1–9, the thumbnails are used to identify buffers for the 'Copy Buffer' command, which is used to transfer a modified spectrum or image in buffer 0, to one of the permanent buffers (1–9).

The (x,y) co-ordinates and intensity (z) values at the position of the cursor in the central display are displayed in the lower left part of the main display. The position is given in both pixel index (lower left corner is pixel (0,0)) and absolute data units. In addition, if the user clicks the left button, the bottom 4 numbers in the lower left positional display execute a cursor-based measurement sequence. Starting from no values being displayed, one left mouse click 'arms' the metrification tool and '–'

is displayed beside d-X, d-Y, dR, d-Z; a second left mouse click at a different point displays the distance between the second and first points (d-X, d-Y, d-R) and the difference in intensities ($Z_2 - Z_1 = d-Z$); a third left mouse click clears d-X, d-Y, d-R, d-Z leaving the cursor information system ready for another metrification use. If the user does not want to be distracted by the continual updating of the side- and lower-panel line-outs, the updating can be turned off by un-selecting the 'z-lines' button at the bottom of the display.

To the right of the main display window an intensity scale, or color bar is displayed which shows the image intensities. The default is gray scale; other color scales can be selected from *Display~Modify Image colors*. The numerical values below and above the intensity scale bar can be used to modify the lower and upper limits of the intensities displayed. Below the color bar there are Y and X limits which can be used to control the range of Y and X (images) or Energy, Intensity (spectra) values that are displayed in the main panel.

2.2. How to download and use aXis2000

Fig. 3 is a screen shot of the internet home page for aXis2000 (<http://unicorn.mcmaster.ca/aXis2000.html>). It provides access to the software via downloading a single file, aXis2000.zip. In order to run aXis2000, it is necessary to have first downloaded IDL which can be obtained from the L3 Harris Geospatial web site. If the user has an IDL license, aXis2000 can be executed from the development environment (idlde.exe). Alternatively, the IDL virtual machine (idlrt.exe) can be used. A desktop shortcut can be set up to start the IDL virtual machine and then aXis2000, as outlined on the aXis2000 web site. The aXis2000 zip file contains all the source files, the executable aXis2000.sav program, and several folders containing data necessary for proper operation. In order to run aXis2000 it is necessary to extract all the content in the aXis2000.

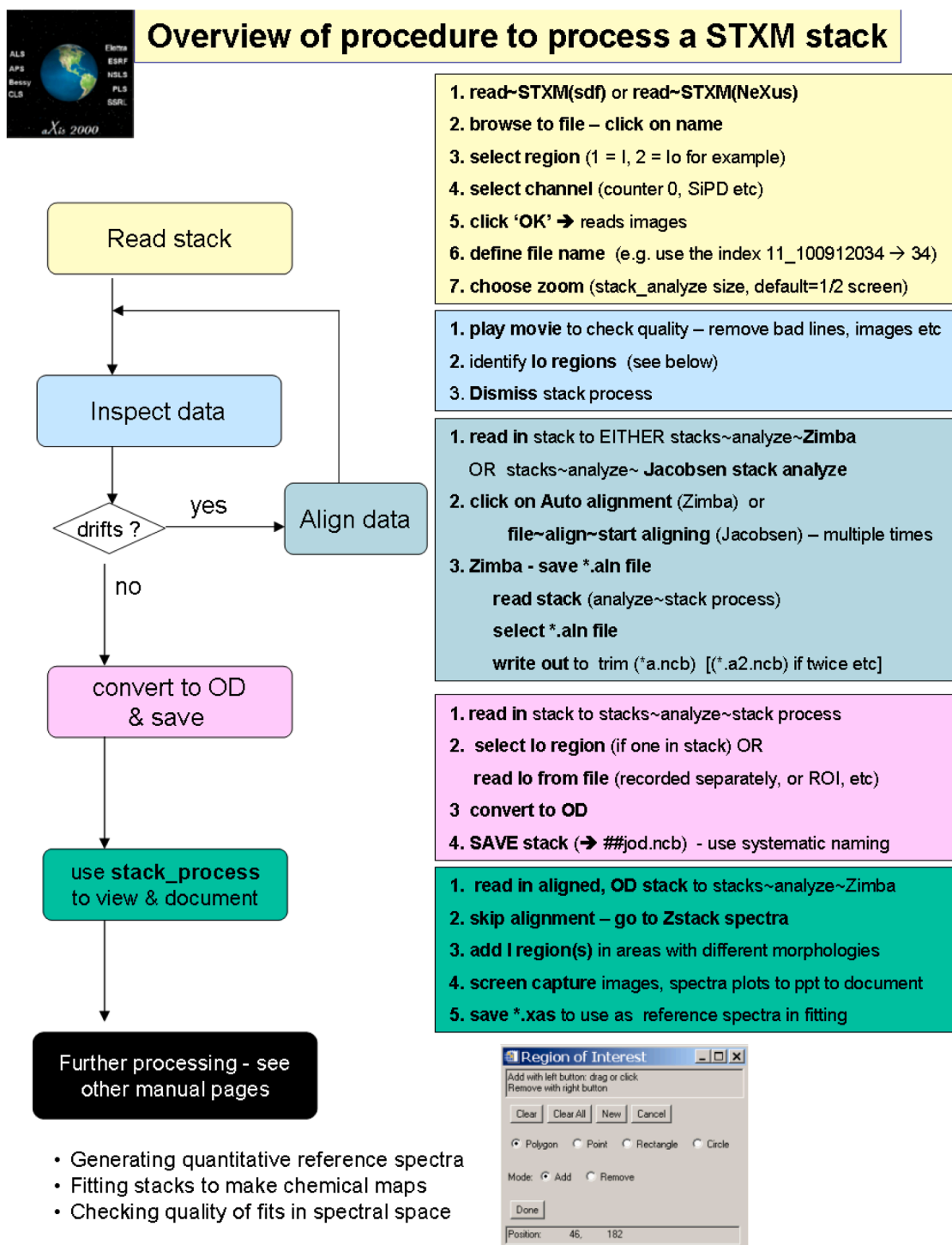


Fig. 5. Workflow for stack analysis. Typical workflow for generating chemical maps from an X-ray spectromicroscopy stack.

zip file, which includes all of the code. There is no cost for aXis2000 as long as it is not commercialized (i.e. the program can not be incorporated into something that is sold). The aXis2000 web site contains several tutorials, which include sample data, and an explanation of how to use aXis2000 to convert the supplied data files to analytically useful results. The site also contains links to a number of documents describing how to use aXis2000 for specific tasks.

2.3. Special features

The processing of stacks and linescan spectra data is a particular strength of aXis2000, since the combined spatial and spectral information in those data types is at the heart of spectromicroscopy. Fig. 4 is a screen shot of the stack_process widget (*Stacks~Analyse~stack process*) which contains 3 main sections: Top left area is used to modify the display; center left area contains commands for modifying the stack; bottom left area is used to output results of stack processing.

aXis2000 has extensive capabilities for reading experimental data

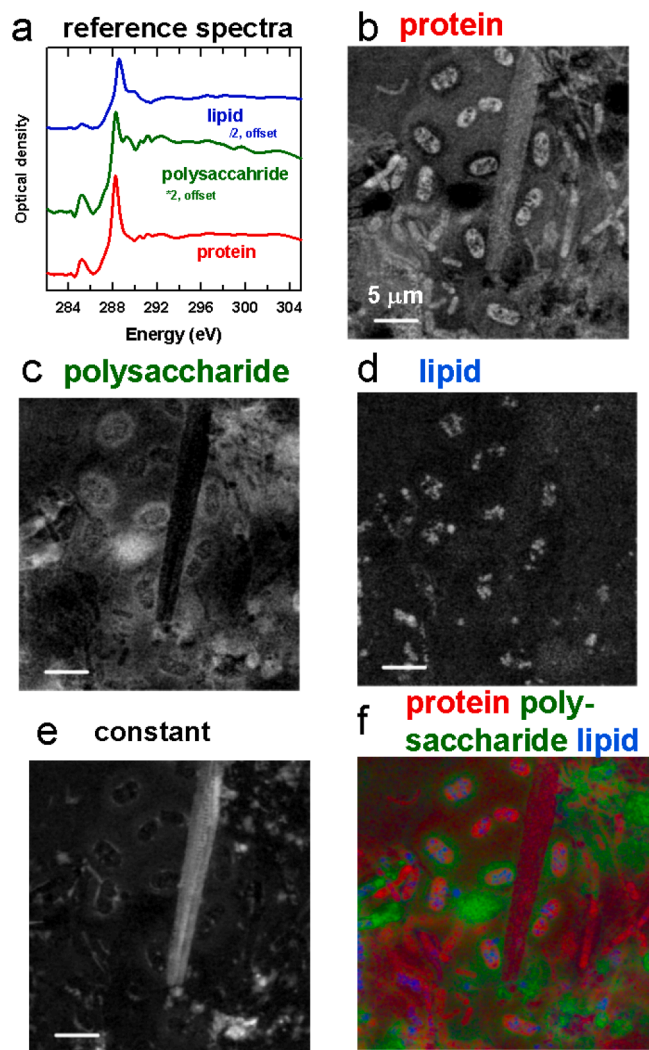


Fig. 6. STXM analysis of a wet biofilm. (a) Reference spectra for 3 main components. Results of quantitative chemical mapping of (b) protein, (c) polysaccharide, (d) lipid and (e) inorganic components of a biofilm from a C 1 s stack. (f) rescaled color coded composite of the protein (red), polysaccharide (green) and lipid (blue) component maps. C 1 s stack measured at ALS “polymer-STXM”, beamline 5.3.2.2 [14].

generated by a wide range of spectromicroscopies. In addition to multiple instances of the four main X-ray spectromicroscopies (scanning transmission X-ray microscopy (STXM), X-ray photoemission electron microscopy (XPEEM), scanning photoelectron X-ray microscopy (SPEM) and transmission X-ray microscopy (TXM)), there are routines to read in 3d (x,y,E) spectromicroscopy data from FT-IR, TEM-XRF, TEM-EELS. The author has worked with the developers of acquisition software and instrument scientists for these various data types in order to make the capabilities of aXis2000 available to many different research communities. In general, the strategy is to read as much as possible from the saved data (absolute spatial co-ordinates; spectral information, (intensities as a function of energy, wavelength, wavenumber); key parameters (dwell time, X-ray polarization, sample information, etc), and convert that information into a standard representation used by aXis2000. Individual spectra are recorded as ascii text files (*.txt, readable by any text editing software). Multi-platform compatible binary stacks, I(x,y,E) and higher dimensional data (e.g. spectro-tomography, I(x,y,E, θ) and X-ray fluorescence yield data, I(x,y,E_{excitation}, E_{emission}) are stored in the IDL multi-platform compatible binary format with an additional *.dat text file which contains values of the

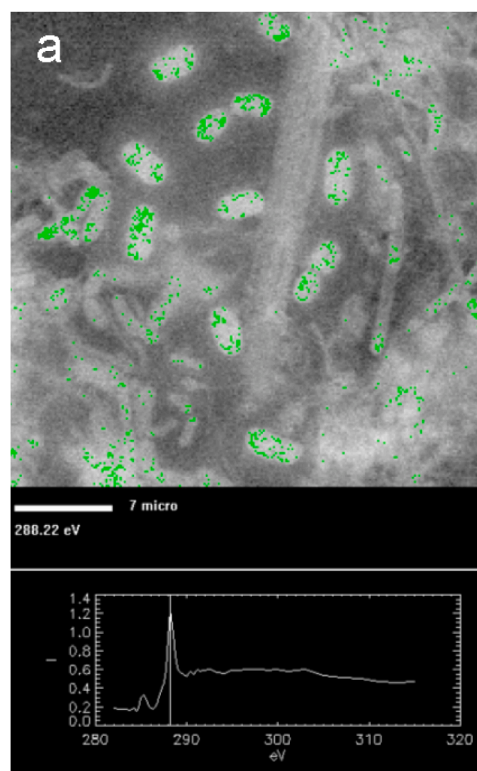


Fig. 7. Verification of quality of a stack fit to the river biofilm (Fig. 6) using masks. (a) Mask of high-protein pixels (thickness of protein > 75 nm; full scale is 175 nm) (green) used to select the displayed spectrum in *stack_process*. (b) Plot of the stack fit of the high-protein spectrum to the protein, polysaccharide and lipid component reference spectra (on an OD1 scale).

parameter axes and other metadata.

When aXis2000 is adapted to read data from a new type of spectromicroscopy or instrument, sample data files are stored in a folder (aXis_pass_test_data) so that routines can be tested as needed as the aXis2000 code evolves. In addition, axis2000-manual web pages are generated in order to explain to users how aXis2000 can be applied to that type of data. Within my time constraints and coding capabilities, aXis2000 can be further extended to read in data from additional types of spectromicroscopies. Please contact the author if that is of interest.

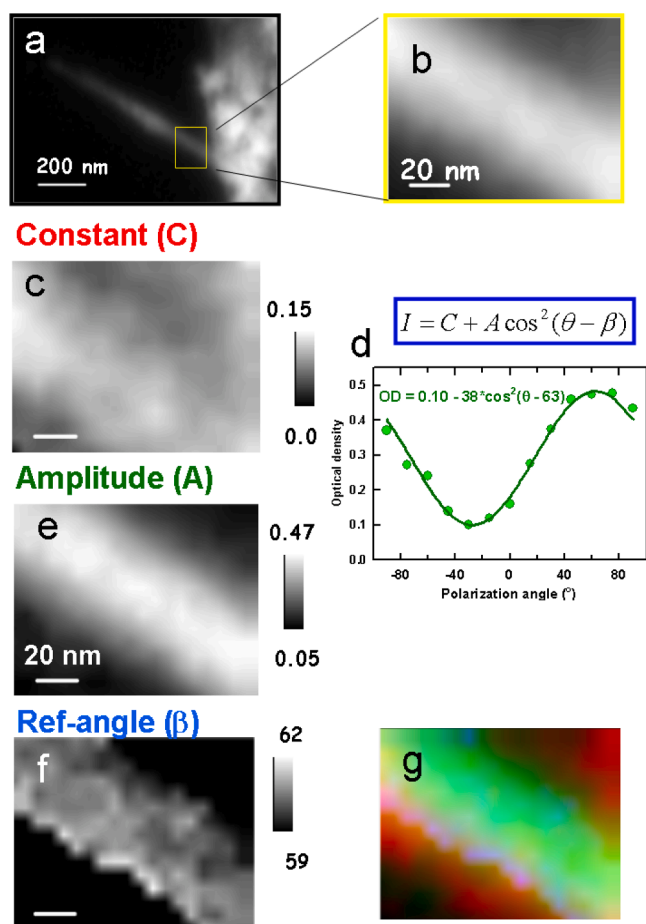


Fig. 8. Example of analysis of spatial distribution of polarization dependence of the C 1s $\rightarrow \pi^*$ transition in an arc discharge carbon nanotube. (a) STXM OD image at 285.2 eV. (b) average of similar images in an area of high quality AD-CNT (yellow box in (a)), measured at 13 different E-vector angles spanning -90° to $+90^\circ$ relative to horizontal. Fitting this polarization stack to the dichroic response function (Eq. 1) yields maps of (c) the constant (C), (d) the amplitude (A) and (e) the reference-angle (β). (f) dichroic signal averaged over the whole AD-CNT (points) in (b) fit to the dichroic response function. (g) color coded composite of the constant, amplitude and reference-angle maps. (CLS ambient-STXM, beamline 10ID1) [17].

2.4. Chemical mapping by least squares fitting STXM stacks

A stack of STXM transmission images can be converted into a set of chemical maps using several different approaches. Fig. 5 outlines a typical workflow for generating chemical maps from X-ray spectromicroscopy stack data. Fig. 6 presents the results for converting a C 1s stack (51 images from 282 to 315 eV) to maps of protein, polysaccharide, lipid and inorganic components [13,14]. The stack (aligned and converted to OD scale), along with quantitative (OD1) reference spectra, is available in the [supplemental information](#) (biofilm-stack_SI.zip). The sample is a wet, riverine biofilm, sandwiched between two X-ray translucent silicon nitride (SiN_x) windows. The stack was measured using the polymer STXM on beamline 5.3.2.2 at the Advanced Light Source (ALS). First, the stack is aligned using Fourier cross-correlation methods (3 different implementations exist in aXis2000). Second, the transmission intensities are converted to optical density (OD) using the spectrum from a suitable non-sample area in the stack (if such an area or areas exist) or recorded separately, before or after the stack. Third, if necessary, the energy scale is calibrated. After each step of the process the user should save the converted stack. In a typical analysis the saved data sets (each, a pair of files: a *.dat text file

with parameters describing the stack, and a *.ncb binary file, containing all the images) might be labeled main, mainj, mainjod, mainjodc, where main is the name of the stack after conversion from the as-recorded stack data using `read~STXM (sdf)`, and additional letter or letters are added to signify alignment (e.g. j for `stacks~Analyze~Jacobsen stack analyse` alignment, which is probably the best, and easiest to use of the 3 alignment codes in aXis2000), OD for conversion to optical density, c for energy calibration, etc.

The next step consists of identifying suitable reference spectra for least squares fitting. In many cases, playing back the OD stack using the movie function in `stacks~stack process` will reveal areas of the sample for which the contrast relative to other areas differs at specific photon energies. Such stacks ‘flash’ or ‘flicker’ when played back, which is a sign of spectroscopic and thus chemical (or dichroic) contrast. (Stacks which simply ‘breathe’ – get more then less intense – have similar spectroscopy at all pixels).

The spectrum of the changing areas can be extracted, saved, and used as one of a set of reference spectra. Alternatively, if the chemical constituents are known and available, their X-ray absorption spectra can be measured using STXM or a non-imaging spectroscopy system. A third possibility is to use multivariate statistical analysis (MSA) methods to identify the number of statistically valid components, and then to extract the reference spectra of the components using multivariate statistical methods. While a 2005 version of the Jacobsen PCA_GUI is implemented in aXis2000 (`stacks~statistical methods~PCA_GUI`), it is recommended to use the Mantis software [10], which is easier to use and contains features such as non-negative matrix methods, not available in the Jacobsen 2005 PCA_GUI code.

Once suitable reference spectra have been obtained, the aligned, calibrated OD stack can be fit with 2 different routines, `stacks~maps~SVD` and `stacks~maps~stack fit`. Both of these routines use the singular value decomposition (SVD) method [15]. SVD is a single pass matrix approximation to a formal least squares fit, which is fast and accurate in situations like X-ray spectromicroscopy where the system of linear equations describing the stack is highly over-determined (typically less than 10 statistically valid components can be extracted from fitting a stack which may contain many thousands of spectra). SVD fit uses only the reference spectra provided by the user. Stack fit uses the user-supplied reference spectra plus a constant. The constant may be needed to account for: (i) an offset of the stack OD scale (as occurs when the I and I_o scales differ by a scale factor), or (ii) one or more chemical components in the area measured do not contain the element whose edge is measured. In the example for which results are presented in Fig. 6, stack fit was used with the C 1s spectra of protein, polysaccharides and lipids as reference spectra (Fig. 6a), to convert the measured C 1s stack to component maps of these three major biomolecular components (Fig. 6b,c,d), plus a constant map (Fig. 6e). The latter maps the SiO₂ skeleton of a diatom, some potassium crystals, and a calcium carbonate shell around some of the bacteria [14]. Fig. 6f is a rescaled color composite of the protein, polysaccharides and lipid component maps. Such color composites are very useful to explore spatial correlations of the chemical components. With more extensive analysis seven different components can be mapped from this data set. In addition, the component maps can be put on a quantitative basis by using reference spectra placed on absolute intensity scales (optical density per nm thickness at normal densities, OD1) [16]. The raw data and selected processing results for this example (and other examples presented) are provided in the [supplemental information](#).

It is important to examine the quality of a candidate stack analysis in the spectral domain, since an arbitrary set of spectra will give some type of fit to any given stack. An example of a spectral domain fit is given in Fig. 7. The high-protein pixels indicated in green in Fig. 7A were identified by applying `Images~generate mask~threshold~histogram` to the protein map (Fig. 6b). The spectrum of those pixels was extracted and a stack fit applied (`spectra~Curve fit~linear regression =stack fit`) using the reference spectra displayed in Fig. 6a, converted to OD1.

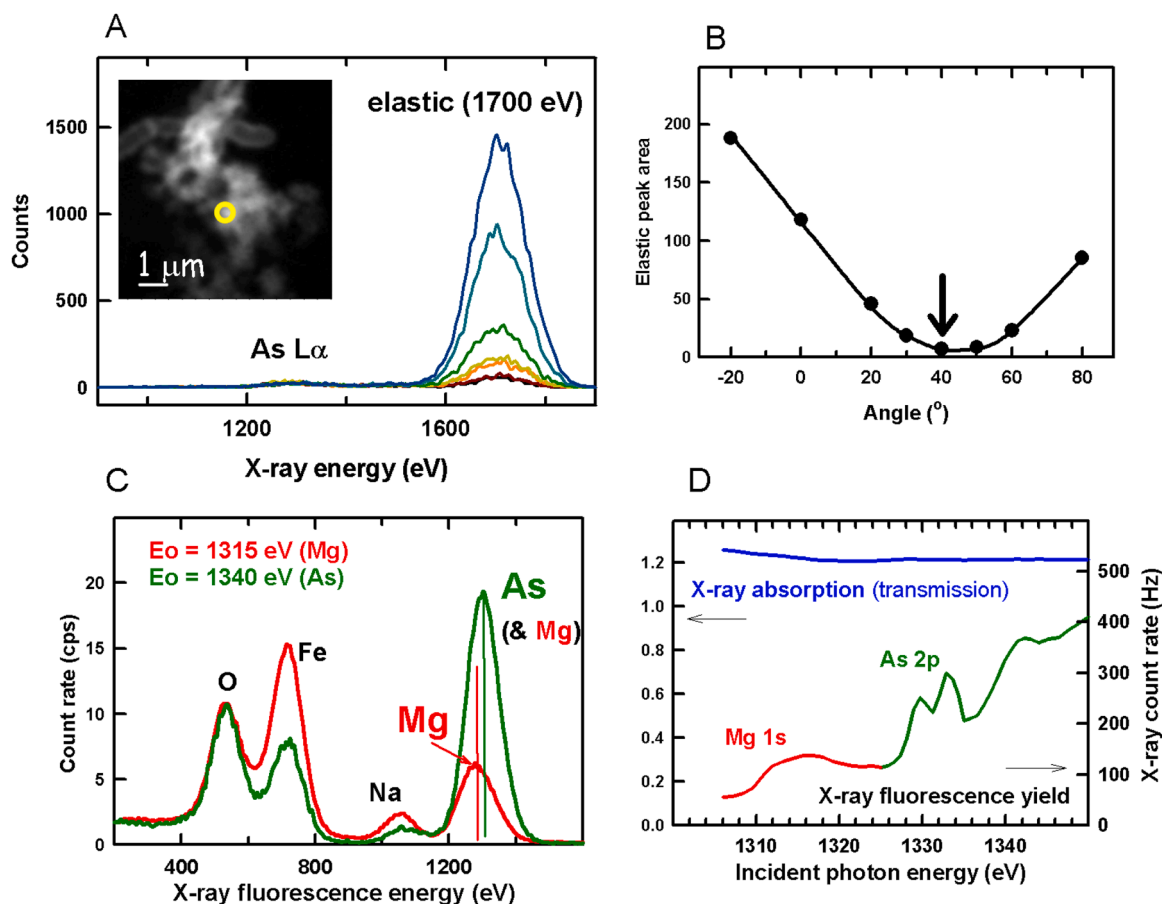


Fig. 9. Analysis of an As-tolerant bacterial biofilm by soft X-ray fluorescence (XRF). (a) Polarization dependence of the X-ray fluorescence spectrum recorded on an As-rich spot of the sample. Note the importance of placing the XRF detector along the direction of the electric vector of the X-rays when making XRD-yield detection in the soft X-ray where the typical ~100 eV wide fluorescence lines mean that the elastic (Rayleigh) scattering overlaps the X-ray fluorescence yield signal in the threshold region which contains the critical near-edge signal useful for identifying chemical states (e.g. differentiating As(III) and As(V) oxidation states). (b) Comparison of XRF-yield mapping and transmission detected X-ray absorption. (ALS, MES-STXM, beamline 11.0.2; CLS 10ID1) [32].

2.5. Polarization methods – XMCD, XLD

Fig. 8 presents results of an aXis2000 analysis of the linear dichroism of an arc discharge multiwall carbon nanotube (AD-MWCNT), measured using the ambient STXM at the spectromicroscopy (SM) beamline at the Canadian Light Source [17]. The source point for the SM beamline is an Apple-II elliptically polarizing undulator (EPU) in which each of the 4 girders supporting the magnet array can be displaced relative to the other three, which allows the linear polarization vector of the light to be oriented over a full 180° range, and thus to seek both maxima and minima of the linear dichroic response [18].

X-ray linear dichroic (XLD) stack maps at 278 eV and 285.2 eV were measured at a number of different orientations of the electric vector relative to the long axis of the AD-MWCNT. Fig. 8a is an image of the AD-MWCNT at 285.2 eV the maximum of the C 1s → π* transition. In a perfect carbon nanotube structure the signal is maximum when the E-vector is aligned perpendicular to the carbon nanotube (CNT) and zero when the E-vector is parallel to the CNT [17,19]. In fact, this is only true in the absence of defects or impurities. Thus, quantitative analysis of the spatial variation of the linear dichroic signal of a CNT provides a way to map defect densities, and thus evaluate the quality of CNT [17]. In this case, the image indicates there is an impurity region toward the central region of the AD-MWCNT, while regions on each side exhibit a more perfect structure. The area imaged in Fig. 8a was measured at 285.2 eV at 13 dichroic angles spanning -90° to +90° relative to the long axis of the AD-MWCNT. The average of these 13 images in the region indicated by the yellow box in Fig. 8a is shown in Fig. 8b. aXis2000 provides a tool

(stacks~maps~polarization fit) to do a pixel-by-pixel fit of this type of dichroic stack to the function:

$$I = C + A \cos^2(\theta - \beta) \quad (1)$$

where C is a constant (no dichroism), A is the amplitude of the dichroism, and β is the angle between the E-vector direction and horizontal at the angle of strongest +ve dichroic signal. Figs. 8c, 8e, and 8f are the maps of C, A and β parameters generated by the polarization stack fit. Fig. 8d is the fit to the average spectrum of the AD-MWCNT. Fig. 8g is a color coded composite of the constant, amplitude and reference angle maps. This approach was used to evaluate the dichroism and thus structural quality of arc discharge (AD) and chemical vapor deposition (CVD) CNT, quantifying the greater structural perfection of the AD relative to the CVD carbon nanotube [17]. The polarization stacks for both AD-CNT and CVD-CNT, and expected outputs are available in supplemental information (CNT_polarization-fit-SI.zip). STXM mapping of linear dichroism was also used to understand organization of protein β-sheets in spider silk dry [20,21] as a function of humidity [22].

2.6. X-ray fluorescence mapping and XRF-yield NEXAFS

Spectral $I(x,y,E)$ or polarization $I(x,y,\theta_{\text{polarization}})$ stacks are an example of 3D data cubes. However there are more dimensions that can be, and have been measured in a spectromicroscopy context, including spectro-tomography ($I(x,y,\theta_{\text{polar}},E)$) [23–25]; spectro-ptychography-to-mography ($I(x,y,\theta_{\text{polar}},E)$) [26,27], laminography ($I(x,y,\theta_{\text{azimuthal}})$) [28]; time ($I(x,y,t)$), and other control parameters such as electrochemical

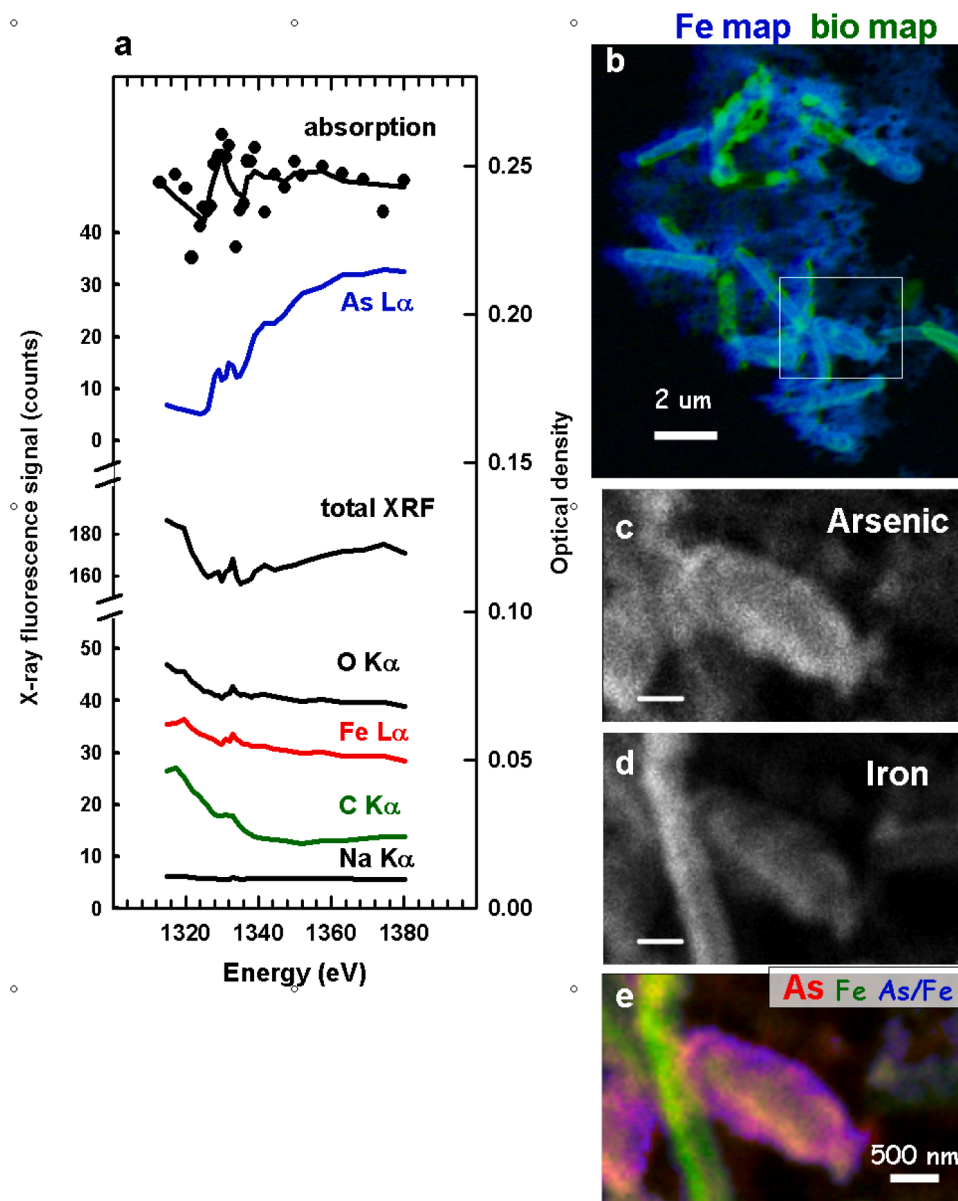


Fig. 10. XRF-yield spectroscopy and elemental mapping of As and Mg in a BoFeN1 biofilm. (a) XRF-yield spectra at a single, As-rich point. The apparently inverted spectral signals in the total XRF and O K α , Fe L α and C K α yields is an example of inverse partial fluorescence yield (IPFY, [2011AR&]). (b) Mapping Fe and biological (Fe L pre-edge) signals. (c) As XRF map. (d) Fe L α map. (e) ratio of the As to the Fe map. (ALS 11.02, CLS 10ID1). [adapted from ref. [32].

potential. aXis2000 offers a number of tools which can analyze such 4D data sets. Here I describe an example of 4D spectromicroscopy in the form of XRF-yield spectral stacks, $(x, y, E_{\text{XRF}}, E_{\text{inc}})$, where E_{XRF} is the energy of the X-ray fluorescence photon, and E_{inc} is the energy of the incident X-ray photon.

Measuring XRF signals in the soft X-ray (<2000 eV) regime is challenging due to the limited energy resolution of silicon drift detectors (SDD), the very low XRF yield [29] and the difficulty of achieving a large solid angle, due to spatial constraints of soft X-ray microscopes. Despite the challenges, XRF detection in STXMs has been achieved at a number of facilities, including Eletta [30], ALS [31], CLS [32], Petra-III [33], Diamond [34] and Spring-8 [35]. In most cases, a single, high photon energy (2 – 3 keV) is used and XRF spectra are measured at specific points or areas, resulting in a 3D data cube, (x, y, E_{XRF}) . That use of XRF measurements gives improved sensitivity relative to transmission detection, and provides elemental mapping, but does not provide NEXAFS chemical speciation. A more challenging yet more powerful

approach is to measure XRF-yield maps at a sequence of incident photon energies across the X-ray absorption edge of an element of interest, thus generating NEXAFS spectromicroscopy with higher sensitivity than can be achieved with transmission detection [32]. aXis2000 has a number of tools to process such 4D $(x, y, E_{\text{XRF}}, E_{\text{inc}})$ data sets.

Fig. 9 presents results from a soft X-ray fluorescence (XRF) yield study of an As-tolerant bacterial biofilm, labeled BoFeN1 [32]. Fig. 9a plots the X-ray fluorescence spectrum excited by 1700 eV X-rays focused to ~ 60 nm at the yellow spot in the insert image, measured as a function of the angle of the linear polarization vector (θ), relative to horizontal ($= 0^\circ$). The SDD XRF detector was tilted 40° from horizontal. There are very large changes in the intensity of the elastic peak (Rayleigh scattering) as the orientation of the E-vector changes relative to the sample – detector direction. Fig. 9b plots the intensity of the elastic peak at 1700 eV as a function of E-vector angle. The data points are fit to a $\cos^2(\theta - \varphi)$ distribution [6]. The reference angle (φ) is -48° , indicating the maximum elastic scattering occurs when the E-vector is at $\sim 90^\circ$ relative to the

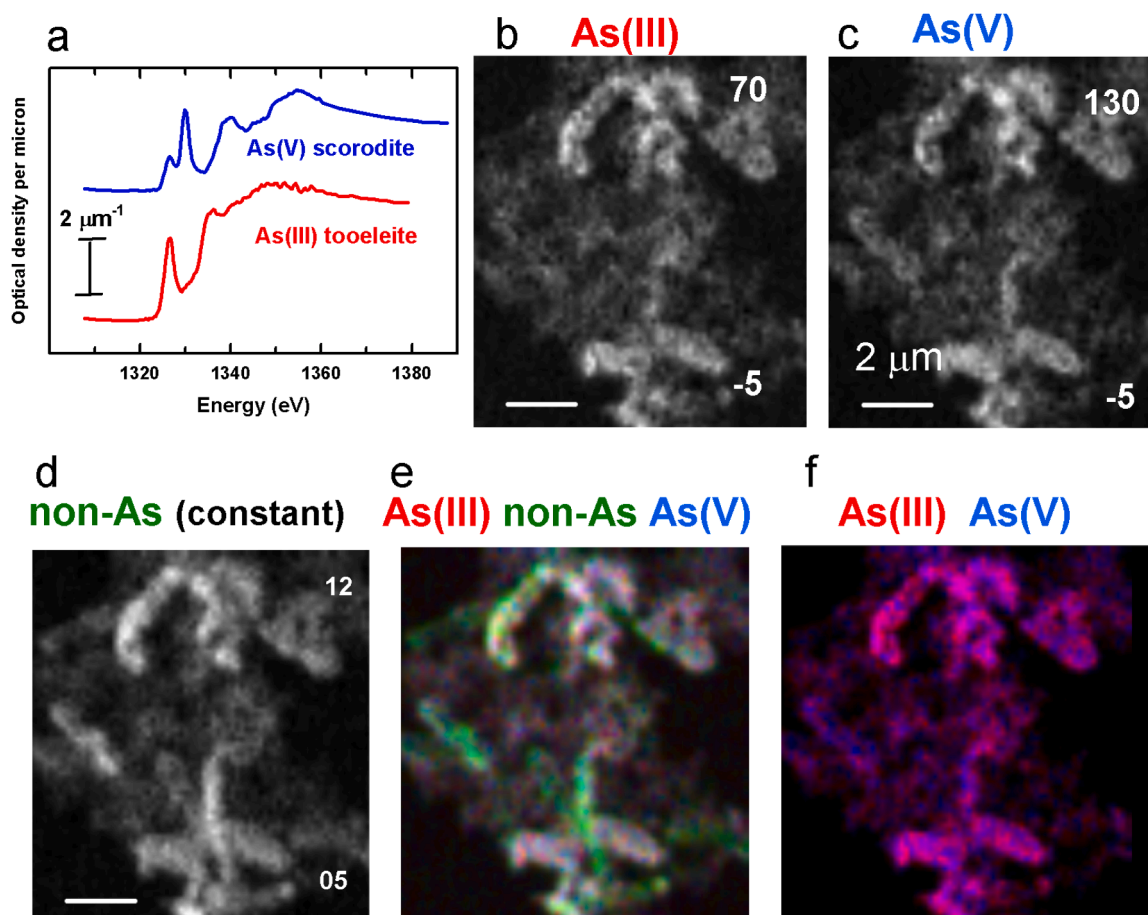


Fig. 11. Chemical mapping of As(III) and As(V) oxidation states in a BoFeN1 biofilm. (a) As L_3 X-ray absorption spectra as of tooeleite ($\text{Fe}_6(\text{AsO}_3)_4\text{SO}_4(\text{OH})_4 \cdot 0.2 \text{H}_2\text{O}$ - As(III)) and scorodite (FeAsO_4 - As(V)) digitized from Fig. 1 of [38]. The intensity scale was adjusted to match that predicted for $1 \mu\text{m}$ thickness of the elemental composition and density of each species. A constant was then subtracted to zero the signal below the As L_3 onset, to account for the absence of signal at lower energies when detected by As $L\alpha$ XRF-yield. (b) Map of As(III), (c) Map of As(V), (d) map of constant signal (no-As) derived from a stack fit of the As $L\alpha$ XRF-yield stack (XRF energies from 1175 to 1450 eV) to the reference spectra in (a). The gray scale reflects the relative amounts of As(III) and As(V). (e) color coded composite of the maps for As(III) – red, constant (biology & iron) – green, and As(V) – blue. (f) color coded composite of As(III) and As(V) component maps. (CLS 10ID1).

sample-detector direction. While the elastic signal is well separated from the As $L\alpha$ signal when the photon energy is 1700 eV, when the photon energy is lowered to the As L_{23} edge (1325 – 1400 eV) in order to measure spatially resolved XRF-yield NEXAFS spectra, the elastic scattering peak occurs at the incident photon energy and thus overlaps the ~ 100 eV wide As $L\alpha$ XRF peak (1200–1400 eV). This emphasizes the importance of placing the XRF detector along the direction of the electric vector of the X-rays (or equivalently, orienting the E-vector of the incident X-rays to point towards the X-ray fluorescence detector) when making XRF-yield detection in the soft X-ray region. Fig. 9c compares the XRF spectrum at the yellow circle in Fig. 9a, measured with incident photon energies of 1315 eV (peak of the Mg 1 s NEXAFS signal) and 1340 eV (peak of the As 2p NEXAFS signal). The ~ 25 eV shift in the position of the peak of the XRF signal around 1300 eV reflects the changing sensitivity from Mg to As in the absorption spectrum. Fig. 9d compares As $L\alpha$ XRF-yield and transmission detected X-ray absorption spectra measured at the yellow dot in Fig. 9a. The XRF-yield signal, which clearly shows the Mg 1 s and As 2p NEXAFS spectral signals, is much more sensitive than the transmission signal, which shows only a very weak As 2p signal without any detail.

Fig. 10a plots total and element-specific partial XRF-yield spectra recorded at a single, As-rich point of the BoFeN1 sample. The apparently inverted spectral signal in the total XRF and O $K\alpha$, Fe $L\alpha$ and C $K\alpha$ yields is an example of inverse partial fluorescence yield (IPFY) signals [36]. Fig. 10b presents a color coded map of the Fe ($\text{OD}_{710} - \text{OD}_{700}$) signal in

blue and the biological (OD_{710} , Fe L pre-edge) signal in green. The strong association of the BoFeN1 cells and the extra-cellular iron oxides is evident. The XRF-yield NEXAFS study set out to: (i) determine the location of the As, which is normally toxic to bacteria and people [37], particularly in the As(III) oxidation state; (ii) map the oxidation states of the As; and (iii) determine if the As is primarily intra-cellular or extra-cellular.

Fig. 10c is the As $L\alpha$ XRF map while Fig. 9d is the Fe $L\alpha$ XRF map of the area inside the yellow box in Fig. 9b. This area includes a young, rod-like cell with little extra-cellular iron oxide, and an old, probably dead, cell which is heavily encrusted with iron oxide. Fig. 9e is a color-coded map with the As signal in red, Fe signal in green and the As/Fe ratio in blue. These results clearly show that the As is predominantly associated with the extra-cellular iron [32], ruling out hypotheses that involve immobilization and neutralization of the As toxicity by an intra-cellular mechanism; (ii) the As is mainly in the As(V) oxidation state [38].

With aXis2000 it is possible to extract the XRF-yield signal from any portion of the XRF spectra recorded at each incident photon energy and assemble that information into a NEXAFS stack. The NEXAFS XRF-yield stack can then be fit with suitable X-ray absorption reference spectra in order to map the spatial distributions of individual chemical species, such as the As(III) and As(V) oxidation states of the arsenic in the BoFeN1 biofilm sample. Fig. 10 presents results from fitting the As XRF-yield signal from the same area for which XRF elemental analysis is presented in Fig. 10.

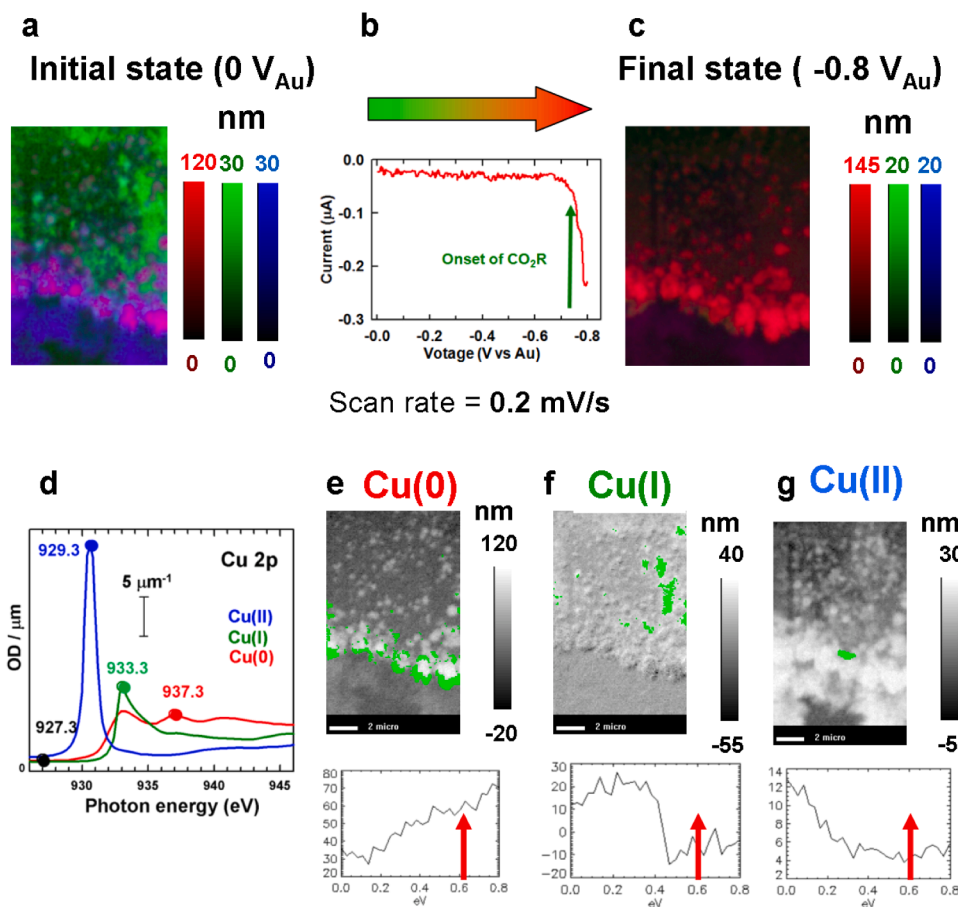


Fig. 12. Example of “chemical movies” derived from stack sequences. (a) Initial distribution of Cu(0), Cu(I) and Cu(II) after electrodeposition from 0.01 M CuSO₄/KCl and change to CO₂ saturated 0.1 M KHCO₃ (red – Cu(0), green = Cu(I), blue = Cu(II); relative). Quantitative mapping by fitting OD1 reference spectra to a 4-energy (4E) Cu L₃ stack. (b) Current during linear sweep voltammetry (LSV) decreasing from 0 V_{Au} to –0.8 V_{Au} at a scan rate of –0.2 mV/s. A total of 30 4E stacks were recorded in ~1 h. (c) distribution of Cu(0), Cu (I) and Cu(II) at –0.8 V_{Au} (red – Cu(0), green = Cu(I), blue = Cu(II); absolute). Conversion to dominantly Cu(0) is evident. The individual component maps are derived by fitting 4E stacks to the intensities at the 4 energies, indicated in (d) (e) potential sequence of maps of Cu(0). The intensity sequence displayed is from the area colored in green, which was the set of pixels that changed the most over the LSV. (f) potential sequence of maps of Cu(I), with signal from those pixels that changed the most. (g) potential sequence of maps of Cu(II), with signal from those pixels that changed the most. The red arrows indicate the onset of CO₂ reduction, as indicated by the rapid change in current. Of significance is the reduction of Cu (II) and Cu(I) to Cu(0) well before the onset of CO₂R at –0.6 V_{Au}. (Bessy-II, MAXYMUS STXM, Feb 2023).

In order to obtain oxidation state maps on a meaningful relative scale, the reference spectra (Fig. 11a) of tooeite (Fe₆(AsO₃)₄.SO₄(OH)₄.0.2 H₂O - As(III)) and scorodite (FeAsO₄ - As(V)) were digitized from [38], intensity scaled to match to that predicted for 1 μm thickness of the elemental composition and density of each species, and a constant subtracted to set the spectral response to zero below the As L₃ onset, to account for the absence of signal at lower energies when As is detected by As L_α XRF-yield. As(III) (Fig. 11b) and As(V) (Fig. 11c) maps were generated by a stack fit to the spectra presented in Fig. 11a.

Stack fit rather than SVD fitting was used, since the system contains many other elements, which have tails in the XRF spectrum that underlie the As L_α signal. The underlying non-As signal is accounted for by the constant (i.e. no As L_α signal) (Fig. 11d) in the stack fit. Fig. 11e and Fig. 11f are color coded composites of the component maps. As shown in a more extended presentation of this analysis in the supplemental (XRF-yield_AsL3_BoFeN_SI.zip), while there is some As(III) and As(V) at each of the bacteria and their associated iron oxide encrustations, the ratio changes at different locations. Overall, when the spectra from As(III)-rich and Fe(V)-rich regions are fit using *Spectra~curve fit~linear regression = stack fit* the As(V) / As(III) ratio changes from 1.2 in the As (III)-rich regions to 2.6 in the As(V)-rich regions. This type of information can only be obtained by measuring the XRF spectral maps at many photon energies through the As L₃ NEXAFS region since the ~150 eV spectral resolution in the XRF spectra measured with a silicon drift detector cannot differentiate As(III) and As(V).

For this study aXis2000 was used extensively. First, the initial stack read-in routine, *read~STXM (sdf)*, was used to extract 3D stacks consisting of the XRF-yield signal of a given element from a pre-selected ROI of the XRF spectrum measured at each position, and incident photon energy, which the STXM_control acquisition program stores in a specific data channel. Second, the *stacks~analyse~XRF stack of stacks* routine of

aXis2000 allows the user to select slices of the full 4D data set (*.ssb). Both XRF-stacks at a fixed incident energy and NEXAFS stacks, over a range of XRF energies can be extracted.

3. Critique and future developments

aXis2000 has provided a continually evolving platform for spectromicroscopy data analysis which has been a useful tool to my group and many other researchers. Relative to some other X-ray spectromicroscopy data analysis packages (e.g. Mantis), it is more difficult to learn to use effectively, due to the complex menu structure and the lack of a guiding ‘work-flow’ architecture. However the ability to process data from many different types of spectromicroscopies (not just soft X-ray microscopes), and the co-ordination of simultaneous analyses in both the spatial and spectral domains, are significant strengths.

3.1. Limitations & how they could be addressed

A feature that is implemented to only a limited extent is a macro capability – linking together sequences of processing steps to make an automated workflow. In principle running IDL in licensed mode is an excellent platform for developing macros, since IDL is both an interpreted and a compiled language. Incorporating virtually any IDL code into aXis2000 is straight forward, and I welcome such additions. If you wish to put your code into the aXis2000 platform, or modify / correct / improve existing aXis2000 routines, please send me an email with the code attached. The parameters needed to execute individual processing steps are already in the call line, or are easily incorporated into the procedure or function calls of individual routines. Thus sequences of routines, plus a skeleton routine to link them together, can be quickly constructed. However, directly incorporating a macro capability into

aXis000 for IDL virtual machine use (unlicensed use of IDL) is more difficult.

As an example, my group recently developed an acquisition protocol to rapidly measure few-energy stacks in a repetitive manner while an external parameter is scanned. In this case the external parameter was the potential applied to an *in-situ* electro-catalysis device driving a CO₂ reduction reaction [39]. To manually process the 30–50 stacks measured in a ~1 h period individually would be very tedious. Thus a macro routine was put together and embedded in aXis2000 (*Stacks_maps_chemi_movie*) which, without user intervention, (i) converts the as-recorded (*.sdf) stack to the internal stack format (*.ncb); (ii) uses a standard region of interest (ROI) of the stack as Io to convert from transmission to absorption; (iii) calibrates the energy scale; (iv) fits each stack to a standard set of reference spectra (in this case, the Cu L₃ OD1 spectra of Cu, Cu₂O and CuO [40] – Fig. 12d); (v) writes a stack of the time / potential sequence of each chemical species. The parameters needed (file names, ROI, reference spectra filenames, output filenames) are contained in a text file (Cu_CO2R_pot_series.lst, in supplemental) which *Stacks~maps~chemi_movie* reads, and works through the list of input files, executing the individual steps listed above. Typically manually fitting one stack takes 2–3 min. The automated *Stacks~maps~chemi_movie* routine processed thirty 4 energy stacks in ~1 min, producing three “chemi-movies” (stacks where the control parameter is potential (or time) rather than photon energy) which display the evolution of the Cu, Cu₂O and CuO spatial distributions and quantitative amounts during the course of an electrochemical reaction. Fig. 12 presents details of this 4D analysis. In prior studies, only 4–6 individual potentials were sampled, as the applied potential was changed from 0 V_{Au} to –0.8 V_{Au}, the potential where CO₂ reduction is actively occurring, as indicated by the current (Fig. 12b). A major goal of these studies was to verify the oxidation state of the active catalyst for the CO₂ reduction reaction (CO₂R). Other studies had determined that CO₂R only started at potentials lower than –0.6 V_{Au}. The STXM chemi-movies clearly show that the Cu(I) and Cu(II) present at 0 V are reduced to Cu(0) at least 0.2 eV prior to the onset of CO₂R, confirming that the active catalyst is metallic Cu, a point that is under active discussion.

A powerpoint which plays back the STXM chemi-movies is available in the [supplemental information](#) (Cu-CO₂R_in_situ_STXM-chemi-movies-BessyII-Feb_2023.pptx in the Chemi-movies.zip supplemental file).

4. . Summary

Here I have described the aXis2000 package for spectromicroscopy data analysis and illustrated its capabilities with examples of 3D and 4D data sets. The [supplemental information](#) (see list below) and the tutorial and work-flow content on the aXis2000 web pages (<http://unicorn.mcmaster.ca/aXis2000.html>) provide more detail. Improvements and further evolution of this package are possible. I encourage those who find value in aXis2000 and have an aptitude for coding, to consider getting involved in improving existing code and writing new content to extend its capabilities. I retired in Jan 2021 at the age of 70. While I am still research active and continue to improve aXis2000, it is time for the next generation to take over.

Declaration of Competing Interest

The authors declare that they have no known competing financial interests or personal relationships that could have appeared to influence the work reported in this paper.

Data availability

Data presented in the article is available in the supplemental information or on request. The software package, manuals et are free and available at <http://unicorn.mcmaster.ca/aXis2000.html>.

Acknowledgements

I thank all the people who have contributed to aXis2000, including **Chris Jacobsen**, who provided many of the stack analysis tools; my son, **Peter Hitchcock** while a high school student (he is now a professor at Cornell) who helped set up the basic widget structure; **Carl Zimba** who supplied ZSTACK and extensively improved the overall package in 2000; **Eli Rotenberg**, **Jonathan Denlinger**, **Stefano Cerasari**, **Tolek Tyliczszak**, **Andreas Scholl**, **Göran Johansson**, **Jacob Stewart OrNSTEIN**, and many others. Special thanks to **Chris Jacobsen** (Stony Brook, NLS-1) for sharing his stack_analyze and pca_gui codes, **Rick Knedler**, for providing the basis for the stack-fit routine, and **Billy Loo** for providing the “SF” X-ray spectral predictor based on the Henke mass absorption coefficients, and the Conjugate Gradient Optimization spectral fitting routine (ax_cgo). This research was funded by the Natural Sciences and Engineering Research Council of Canada, and a tier 1 Canada Research Chair in Materials Research (2000–2016). Results presented were measured at the Advanced Light Source (supported by the Director, Office of Energy Research, Office of Basic Energy Sciences, Materials Sciences Division of the U.S. Department of Energy), The Canadian Light Source (supported by the Canadian Foundation for Innovation), and Bessy-II (Maxymus beamline, operated by the Helmholtz-Zentrum Berlin für Materialien und Energie).

Supplemental Information

- * aXis2000-manual.pdf (08-May-2023).
- * Zimba-manual.pdf.
- * Biofilm C 1 s stack (biofilm-stack_SI.zip).
- * CNT dichroic stack (CNT_polarization-fit-SI.zip).
- * As_biofilm_XRF-yield stack (XRF-yield_AsL3_BoFeN_SI.zip).
- * STXM Chemi-movies (Chemi-movies.zip).

Appendix A. . Supporting information

Supplementary data associated with this article can be found in the online version at [doi:10.1016/j.elspec.2023.147360](https://doi.org/10.1016/j.elspec.2023.147360).

References

- [1] ([https://en.wikipedia.org/wiki/IDL_\(programming_language\)](https://en.wikipedia.org/wiki/IDL_(programming_language))) (accessed 17-Apr-2023).
- [2] D. Attwood, *Soft X-rays And Extreme Ultraviolet Radiation. Principles and Applications*, Cambridge University Press., 1999.
- [3] C. Jacobsen, S. Wirick, G. Flynn, C. Zimba, *Soft X-ray Spectroscopy from Image Sequences with Sub-100 nm Spatial Resolution*, *J. Microsc.* 197 (2000) 173–184.
- [4] H. Ade, A.P. Hitchcock, NEXAFS microscopy and resonant scattering: Composition and orientation probed in real and reciprocal space, *Polymer* 49 (2008) 643–675.
- [5] A.P. Hitchcock, *Soft X-ray spectromicroscopy and ptychography*, *J. Electron Spectrosc. Relat. Phenom.* 200 (2015) 49–63.
- [6] C.J. Jacobsen, *X-ray Microscopy*, Cambridge University Press., 2019.
- [7] W.H. Press, B.P. Flannery, S.A. Teukolsky and W.T. Vetterling, *Numerical Recipes in C: The Art of Scientific Computing* (Cambridge University Press, 1992).
- [8] C.A. Schneider, W.S. Rasband, K.W. Eliceiri, *NIH Image to ImageJ: 25 years of image analysis*, *Nat. Methods* 9 (2012) 671–675.
- [9] F. Zeitvogel, M. Obst, *ScatterJn: an imagej plugin for scatterplot-matrix analysis and classification of spatially resolved analytical microscopy data*, *J. Open Res. Softw.* 4 (2016) e5.
- [10] M. Lerotic, R. Mak, S. Wirick, F. Meirer, C. Jacobsen, *MANTIS: a program for the analysis of X-ray spectromicroscopy data*, *J. Synchrotron Radiat.* 21 (2014) 1206–1212.
- [11] B. Watts, J. Raabe, *A NeXus/HDF5 based file format for STXM*, *AIP Conf. Proc.* 1696 (2016), 020042.
- [12] J. Wu, M. Lerotic, R. Leary, S. Collins, Z. Saghi, P. Midgley, V. Berejnov, D. Susac, J. Stumper, G. Singh, A.P. Hitchcock, *Optimization of Three-Dimensional (3D) chemical imaging by soft X-ray spectro-tomography using a compressed sensing algorithm*, *Microsc. Microanal.* 23 (2017) 951–956.
- [13] J.R. Lawrence, G.D.W. Swerhone, G.G. Leppard, T. Araki, X. Zhang, M.M. West, A. P. Hitchcock, *Scanning transmission X-ray, laser scanning, and transmission electron microscopy mapping of the exopolymeric matrix of microbial biofilms*, *Appl. Environ. Microbiol.* 69 (2003) 5543–5554.
- [14] A.P. Hitchcock, C. Morin, X. Zhang, T. Araki, J.J. Dynes, H. Stöver, J.L. Brash, J. R. Lawrence, G.G. Leppard, *Soft X-ray spectromicroscopy of biological and*

- synthetic polymer systems, *J. Electron Spectrosc. Relat. Phenom.* 144–147 (2005) 259–269.
- [15] I.N. Koprinarov, A.P. Hitchcock, C. McCrory, R.F. Childs, Quantitative mapping of structured polymeric systems using singular value decomposition analysis of soft x-ray images, *J. Phys. Chem. B* 106 (2002) 5358–5364.
- [16] A.P. Hitchcock, *Soft X-ray Imaging and Spectromicroscopy* Chapter 22 in Volume II of the Handbook on Nanoscopy, eds. Gustaaf Van Tendeloo, Dirk Van Dyck and Stephen J. Pennycook, Wiley, 2012, pp. 745–791.
- [17] E. Najafi, D. Hernández Cruz, M. Obst, A.P. Hitchcock, B. Douhard, J.-J. Pireaux, A. Felten, Polarization dependence of the C 1s X-ray absorption spectra of individual multi-walled carbon nanotubes, *Small* 4 (2008) 2279–2285.
- [18] K.V. Kaznatcheyev, Ch Karunakaran, F. He, M. Sigrist, T. Summers, M. Obst, A. P. Hitchcock, CLS ID-10 chicane configuration: from "simple sharing" to extended performance with high speed polarization switching, US Synchrotron Radiation Instrumentation, April 2007, Baton Rouge, LA, Nucl. Inst. Meth A582 (2007) 103–106.
- [19] S. Banerjee, T. Hemraj-Benny, S. Sambasivan, D.A. Fischer, J.A. Misewich, S. S. Wong, Near-edge X-ray absorption fine structure investigations of order in carbon nanotube-based systems, *J. Phys. Chem. B* 109 (2005) 8489.
- [20] D. Hernández Cruz, A.P. Hitchcock, M.M. West, M.-E. Rousseau, M. Pézolet, Quantitative mapping of the orientation of fibroin β -sheets in *B. mori* cocoon fibers by scanning transmission X-ray microscopy, *Biomacromolecules* 7 (2006) 836–843.
- [21] M.E. Rousseau D. Hernández Cruz M.M. West A.P. Hitchcock M. Pézolet Nephilia clavipes Spider Dragline Silk Microstructure Studied by Scanning Transmission X-Ray Microscopy *J. American Chemical Society* 2007 3897 3905.
- [22] T. Lefevre, M. Pézolet, D. Hernández Cruz, M.M. West, M. Obst, A.P. Hitchcock, C. Karunakaran, K.V. Kaznatcheyev, Mapping molecular orientation in dry and wet dragline spider silk, *J. Phys. Conf. Ser.* 186 (2009), 012089.
- [23] G.A. Johansson, T. Tyliczszak, G.E. Mitchell, M. Keefe, A.P. Hitchcock, Three dimensional chemical mapping by scanning transmission X-ray spectromicroscopy, *J. Synchrotron Radiat.* 14 (2007) 395–402.
- [24] M. Obst, J. Wang, A.P. Hitchcock, Soft X-ray spectro-tomography study of cyanobacterial biomineral nucleation, *Geobiology* 7 (2009) 577–591.
- [25] G. Schmid, M. Obst, J. Wu and A.P. Hitchcock, 3D chemical imaging of nanoscale biological, environmental and synthetic materials by soft X-ray spectro-tomography, Chapter 2 in *X-ray and Neutron Techniques for Nanomaterials Characterization*, Vol. 5., C.S.S.R. Kumar, ed. (2016) 43 – 94 (Springer, Berlin, 2016) ISBN 978-3-662-48606-1.2.
- [26] J. Wu, X.H. Zhu, D.A. Shapiro, J.R.I. Lee, T. van Buuren, M.M. Biener, S. A. Gammon, T.T. Li, T.F. Baumann, A.P. Hitchcock, 4D imaging of ZnO coated alumina aerogels by scanning transmission X-ray microscopy andptychographic tomography, *J. Phys. Chem. C* 122 (2018) 25374–25385.
- [27] H. Yuan, Hui Yuan, T. Casagrande, D. Shapiro, Y.-S. Yu, B. Enders, J.R.I. Lee, T. Van Buuren, M.M. Biener St., A. Gammon, Th.F. Baumann, A.P. Hitchcock, 4D Imaging of ZnO-Coated Nanoporous Al₂O₃ aerogels by chemically-sensitive ptychographic tomography: implications for designer catalysts, *ACS Appl. Nanomater.* 4 (2021) 621–632.
- [28] K. Witte, A. Späth, S.Finizio, C. Donnelly, B. Watts B, B. Sarafimov B, From 2D STXM to 3D imaging: soft X-ray laminography of thin specimens, *Nano Lett.* 20 (2020) 1305–1314.
- [29] M.O. Krause, Atomic radiative and radiationless yields for K and L Shells, *J. Phys. Chem. Ref. Data* 8 (1979) 307.
- [30] A. Alberti, T. Klatka, A. Longoni, D. Bacescu, A. Marcello, A. De Marco, A. Gianoncelli, A. Kaulich, Development of a low-energy x-ray fluorescence system with sub-micrometer spatial resolution, *X-ray Spectrom.* 38 (2009) 205–210.
- [31] A.P. Hitchcock, T. Tyliczszak, M. Obst, G.D.W. Swerhone, J.R. Lawrence, Improving sensitivity in soft X-ray STXM using low energy X-ray fluorescence, *Microsc. Microanal.* 2 (2010) 924–925.
- [32] A.P. Hitchcock, M. Obst, J. Wang, Y.S. Lu, T. Tyliczszak, Advances in the detection of as in environmental samples using low energy X-ray fluorescence in a scanning transmission X-ray microscope: arsenic immobilization by an Fe(II)-oxidizing freshwater bacteria, *Environ. Sci. Technol.* 46 (2012) 2821–2829.
- [33] K. Andrianov, A. Haidl, L. Lühl, A. Dehlinger, H. Dierks, R. Gnewkow, T. Nisius, B. Kanngießler, T. Wilhein, Scanning X-ray microscopy with large solid angle x-ray fluorescence detection at the XUV Beamline P04, DESY, *J. Instrum.* 13 (2018). C05013–C05013.
- [34] N.N. Mahmoud, M. Harfouche, A.M. Alkilany, A.G. Al-Bakri, R.A. El-Qirem, S. A. Shraim, E.A. Khalil, Synchrotron-based X-ray fluorescence study of gold nanorods and skin elements distribution into excised human skin layers, *Colloids Surf. B Biointerfaces* 165 (2018) 118–126.
- [35] M. Oura, T. Ishihara, H. Osawa, H. Yamane, T. Hatsui, T. Ishikawa, Development of a scanning soft x-ray spectromicroscope to investigate local electronic structures on surfaces and interfaces of advanced materials under conditions ranging from low-vacuum to helium atmosphere, *J. Synchrotron Rad.* 27 (2020) 664–674.
- [36] A.J. Achkar, T.Z. Regier, H. Wadati, Y.-J. Kim, H. Zhang, D.G. Hawthorn, Bulk sensitive x-ray absorption spectroscopy free of self-absorption effects, *Phys. Rev. B* 83 (2011), 129901.
- [37] E. Marie Muehe, L. Scheer, B. Daus, Andreas Kappler, Fate of arsenic during microbial reduction of biogenic versus Abiogenic As–Fe(III)–Mineral Coprecipitate, *Environ. Sci. Tehcnology* 47 (2013) 8297–8307.
- [38] K. Benzerara, G. Morin, T.H. Yoon, J. Miot, T. Tyliczszak, C. Casiot, O. Bruneel, F. Farges, G.E. Brown, Nanoscale study of as biomineralization in an acid mine drainage system, *Geochim. Et. Cosmochim. Acta* 72 (2008) 3949–3963.
- [39] C. Zhang, H. Eraky, P. Ingino, M. Obst, J. Wang, D. Higgins and A.P. Hitchcock, In-situ STXM Characterization of Cu/Cu₂O Electrocatalysts for CO₂ Reduction, *X-ray Microscopy 2022, Taiwan, 19–24 Jun 2022. AIP Conference Proceedings (2023) in press.*
- [40] P. Jiang, D. Prendergast, F. Borondics, S. Porsgaard, L. Giovanetti, E. Pach, J. Newberg, H. Bluhm, F. Besenbacher, M. Salmeron, Experimental and theoretical investigation of the electronic structure of Cu₂O and CuO thin films on Cu (110) using x-ray photoelectron and absorption spectroscopy, *J. Chem. Phys.* 138 (2013), 024704.
- [41] T. Harasztí, M. Grunze, M.G. Anderson, STXMPy: a new software package for automated region of interest selection and statistical analysis of XANES Data, *Chem. Cent. J.* 4 (2010) 11.
- [42] T. Henn (2023). STXM data analysis script collection - STACKLab (<https://www.mathworks.com/matlabcentral/fileexchange/24006-stxm-data-analysis-script-collection-stacklab>), MATLAB Central File Exchange. Retrieved January 1, 2023.
- [43] M. Marcus, Data analysis in spectromicroscopy, *J. Electron Spectrosc. Rel. Phen.* 264 (2023), 147310.
- [44] L. Yijin, F. Meirer, P.A. Williams, J. Wang, J.C. Andrews, P. Pianetta, TXM-Wizard: a program for advanced data collection and evaluation in full-field transmission X-Ray Microscopy, *J. Synchrotron Radiat.* 19 (Pt 2) (2012) 281–287.
- [45] M. Basham, J. Filik, M.T. Wharmby, P.C.Y. Chang, B. El Kassaby, M. Gerring, J. Aishima, K. Levik, B.C.A. Pulford, I. Sikharulidze, et al., *Data Analysis Workbench (DAWN)*, *J. Synchrotron Rad.* 22 (2015).
- [46] V.A. Solé, E. Papillon, M. Cotte, Ph Walter, J. Susini, A multiplatform code for the analysis of energy-dispersive X-ray fluorescence spectra, *Spectrochim. Acta Part B* 62 (2007) 63–68. (<http://www.sciencedirect.com/science/journal/05848547>).
- [47] P. Gilbert, Polarization-dependent Imaging Contrast (PIC) Mapping in 2018, *Microsc. Micro* 24 (2018) 454–456.
- [48] M. Osterhoff, J. Goeman, T. Salditt, S. Köster, STXM analysis: preparing to go live @ 750 Hz, *AIP Conf. Proc.* 2054 (2018), 060075.